Nanoscale

Accepted Manuscript

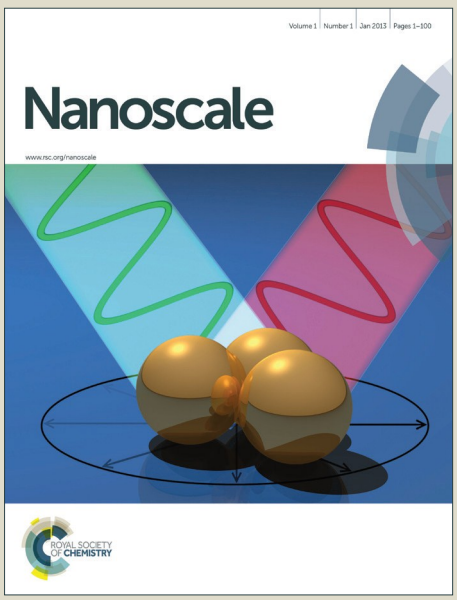

ROYAL SOCIETY OF CHEMISTRY

www.rsc.org/nanoscale

Nanoscale

Dynamic Article Links ►

Cite this: DOI: 10.1039/c0xx00000x

www.rsc.org/xxxxxx

ARTICLE TYPE

Polarized emission from $CsPbX_3$ perovskite quantum dots

Dan Wang[1], Dan Wu[2], Di Dong[1], Wei Chen[1], Junjie Hao[1], Jing Qin[1], Bing Xu[1], Kai Wang[1*], and Xiaowei Sun[1,2]

[1] Department of Electrical and Electronic Engineering, College of Engineering, South University of Science and Technology of China, 1088 Xue-Yuan Road, Shenzhen, Guangdong 518055, China
[2] School of Electrical and Electronic Engineering, Nanyang Technological University, 639798, Singapore

Received (in XXX, XXX) Xth XXXXXXXXX 201X, *Accepted Xth XXXXXXXXX 201X*
First published on the web Xth XXXXXXXXX 201X
DOI: 10.1039/b000000x

Abstract

Compared to the organic/inorganic hybrid perovskite, full inorganic perovskite quantum dots (QDs) exhibit higher stability. In this study, full inorganic $CsPbX_3$ (X=Br, I and mixed halide systems Br/I) perovskite QDs have been synthesized and interestingly, these QDs showed highly polarized photoluminescence which is systematically studied for the first time. Furthermore, the polarization of $CsPbI_3$ was as high as 0.36 in hexane and 0.40 in film. The $CsPbX_3$ perovskite QDs with high polarization properties indicate they possess great potential for applying in new generation display with wide colour gamut and low power consumption.

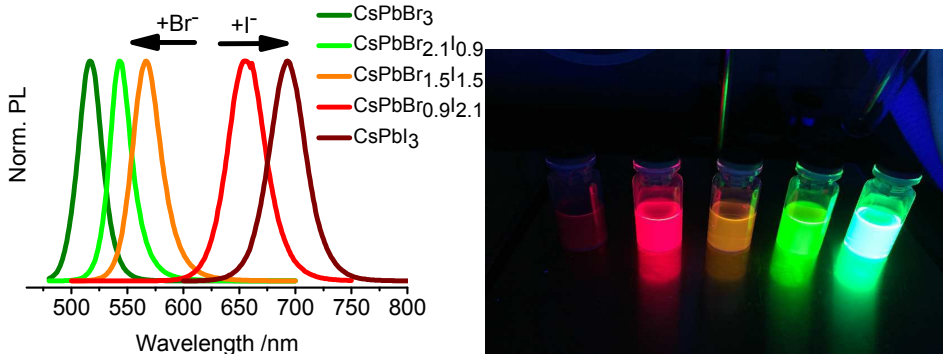

* To whom correspondence should be addressed. E-mail for K. Wang: wangk@sustc.edu.cn, Tel. +86-755-88018181;

1. Introduction

The emerging organic/inorganic hybrid perovskites [1-5], such as $MAPbX_3$ (MA=CH_3NH_3; X=Cl, Br, I) QDs, have attracted much attention due to their excellent performance in solar cells [6] and optical devices. [7] Among these organic/inorganic hybrid perovskites, $MAPbI_3$ has been studied extensively in the field of solar cells since 2009, [8-13] and the power conversion efficiency (PCE) has approached about 20% recently. [14] On the other hand, owing to the wide wavelength tunability (400~800 nm) and narrow band emission with full width at half-maximum (FWHM) of about 20 nm, [10] organic/inorganic hybrid perovskites have been considered as the emissive component in phosphor-converted white-light-emitting diodes (pc-WLED) and electroluminescence (EL) devices for high quality lighting and wide color gamut display. [5,7,10,15] Compared to the organic/inorganic hybrid perovskites, full inorganic perovskite QDs, such as $CsPbX_3$ (X=Cl, Br, I), exhibit higher stability [16] and provide superior photoelectricity performance. [17]

In wide color gamut liquid crystal display (LCD) with quantum dot LEDs as backlight, [18] besides of narrow FWHM, polarized emission is another important and key issue for the backlight source to achieve high system optical efficiency. More than half unpolarized light will be absorbed and lost passing through the two orthogonal polarizers without dual brightness enhancement film (DBEF) (*ie.* lower cost). [19, 20] LCD has been pursuing backlight source with narrow FWHM and strong polarized emission for wide color gamut and low power consumption display. [21] In addition to display applications, polarized emission with precisely controlled peak wavelength has huge potential to be applied in ultra-sensitive photodetector, information storage, etc.

In this study, we discovered that $CsPbX_3$ perovskite QDs emit polarized light either in solution or in film without using extra polarizer. We have synthesized $CsPbX_3$ QDs (X = Br, I and mixed halide systems Br/I) and they show wide wavelength tunability through compositional modulations (500~700 nm), narrow FWHM of 24 nm and high quantum yield (QY) of ~70%. More interestingly, these QDs showed strong polarization property and the polarization of $CsPbI_3$ reached to 0.36 in hexane and 0.40 in film. As far as we know, firstly the polarization property of $CsPbX_3$ perovskites have been observed and studied systematically in this paper. These perovskites possess the potential to be applied in LCD backlight units as polarized emission sources directly for high color-gamut and low power consumption displays.

2. Experimental

2.1 Chemicals

Most chemicals used in the experiments including Cs_2CO_3 (99.99%), octadecene (ODE, 90%), oleic acid (OA), oleylamine (OLA, 70%), PbI_2 (99.999%) and $PbBr_2$ (99.999%) were purchased from Aladdin. The n-hexane (>97.0%) was purchased from Lingfeng Reagent Company (Shanghai, China). All solvents and reagents were of analytical grade and directly used without further purification.

Instrument

X-ray diffraction (XRD) measurements were performed on a X-ray diffractometer (Bruker Advance D8 Ew, Germany) with Cu Kα radiation (λ = 1.54178 Å). The operation voltage and current were 40 kV and 25 mA, respectively. The 2θ range was from 10° to 60° in steps of 0.02°. The transmission electron microscopy (TEM) images were carried out on a FEI Tecnai G2 F30 transmission electron microscope operating at an acceleration voltage of 300 kV. UV–vis absorption spectra and florescence spectra were recorded on a PERSEE TU-1901 spectrophotometer and a Gilden Photonics fluoroSENS spectrofluorometer. Freshly prepared samples in 1 cm quartz cells were used to perform all UV–vis absorption and emission measurements.

2.2 Preparation of Cs-oleate

The preparation process is similar to the previous report by L. Protesescu *et al* [22] with slight revision here. Typically, 0.0814 g Cs_2CO_3 was loaded into a 25 mL 3-neck flask along with 4 mL octadecene, and 0.25 mL OA, dried for 1 h at 120 ºC, and then heated under inert argon gas to 150 ºC until all Cs_2CO_3 reacted with OA.

2.3 Synthesis of $CsPbX_3$ QDs

Firstly, 5 mL ODE, PbX_2 (0.188 mmol) such as 0.087 g PbI_2, 0.069 g $PbBr_2$, 0.5 mL dried OLA and 0.5 mL dried OA were loaded into 25 mL 3-neck flask. They were heated under vacuum for 30 mins at 50 ºC and then heated to the 120 ºC for 1 h. And then the temperature was raised to 180 ºC and Cs-oleate solution (0.4 mL, prepared as described above and preheated before injection) was quickly injected. After 5 s, the reaction mixture was cooled by the ice-water bath to room temperature. The color of the reaction solution changed quickly (yellow-green for $CsPbBr_3$ and crimson for $CsPbI_3$). The crude solutions were separated by centrifugation. The obtained supernatant was discarded and the precipitate was dissolved in hexane to obtained stable colloidal QDs solution of $CsPbBr_3$ or $CsPbI_3$. The synthesis of $CsPbX_3$ QDs possesses the advantages of low preparation cost and easy processing.

2.4 Synthesis of the Mixed $CsPbBr_{3-x}I_x$ QDs

Firstly, ODE (5 mL), mixture reagents (PbI_2 and $PbBr_2$) with different mole ratios, dried OLA (0.5 mL) and dried OA (0.5 mL) were loaded into 25 mL 3-neck flask. They were heated under vacuum for 30 mins at 50 ºC and then heated to the 120 ºC for 1 h. And then the temperature was raised to 180 ºC and Cs-oleate solution (0.4 mL, prepared as described above and preheated before injection) was quickly injected and, 5s later, the reaction mixture was cooled by the ice-water bath to room temperature. The crude solutions were separated by centrifugation and the precipitate was dissolved in hexane.

Figure 1: The synthesis schematic of $CsPbX_3$ QDs

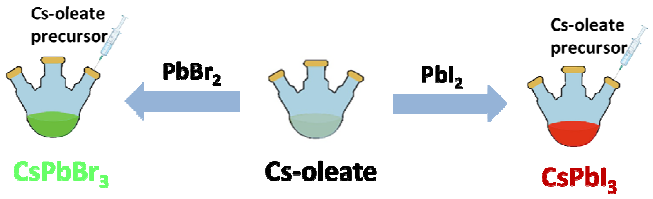

3. Results and Discussion

3.1 Preparation and Structure of the $CsPbX_3$ QDs

The synthesis of $CsPbX_3$ QDs was performed under water-free and oxygen-free conditions. Color changes were observed rapidly after the injection of the Cs-oleate precursor into PbX_2 salt solution (yellow-green for $CsPbBr_3$ and crimson for $CsPbI_3$ shown in Figure 1). The mixed halide perovskite $CsPbBr_{3-x}I_x$ was prepared by the same process, except that appropriate mole ratios of the $PbBr_2$ and PbI_2 salts were used instead.

TEM and energy-dispersive spectroscopy (EDS) were used to detect morphologies and elemental content of $CsPbX_3$ perovskite. The size of $CsPbBr_3$ QDs is 17±0.10 nm seen from Figure 2a-2b and the inset in the top-right is the corresponding selected area electron diffraction (SAED) image of $CsPbBr_3$ QDs. The characteristic diffraction points confirm that the structure of $CsPbBr_3$ QDs belongs to the single crystal cubic phase. The size of $CsPbBr_{1.5}I_{1.5}$ QDs gets slightly larger than that of $CsPbBr_3$ and crystal defects could be observed from the irregular diffraction points in SAED images shown in the Figure 2c-2d. The $CsPbI_3$ QDs have a similar tendency in the crystal structure shown in the Figure 2e-2f. The diffraction images prove that the $CsPbBr_3$ perovskite is of single crystal structure corresponding to the perfect cubic phase and the other two samples have been deviated from the cubic phase.

XRD data in Figure 3 confirm the changes of crystal structure between the $CsPbBr_3$ QDs and $CsPbI_3$ QDs, which the sample with a bigger iodine amount result in a shift moved to the small angle degree. [16] In accordance with the TEM analysis, the $CsPbBr_3$ perovskite belongs to the cubic crystal structure. Other samples, especially the $CsPbI_3$ perovskite, have more or less deviated from the cubic phase. EDS results show Br/Pb atom ratio of $CsPbBr_3$ QDs is 3.5, confirming the presence of Br-rich surface (shown in the Figure S1) in good agreement with the literature. [10, 23, 24] The Br/I atom ratio is 1.3 for the $CsPbBr_{1.5}I_{1.5}$ QDs, almost in consistent with the stoichiometry.

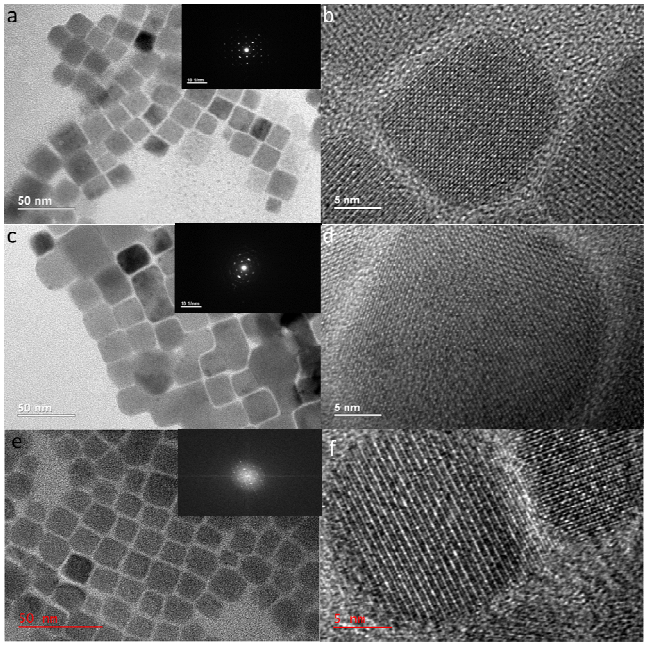

Figure 2: TEM and HR-TEM images of $CsPbBr_3$ (a, b); $CsPbBr_{1.5}I_{1.5}$ (c, d); $CsPbI_3$ (e, f). The insets are the corresponding diffraction images.

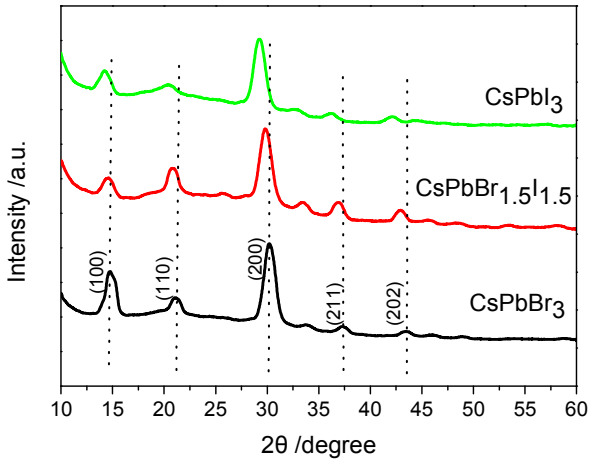

Figure 3: XRD pattern of $CsPbBr_3$; $CsPbBr_{1.5}I_{1.5}$; $CsPbI_3$.

3.2 Optical Properties of the $CsPbX_3$ Perovskite

Figure S2 shows the UV/vis absorption spectra of $CsPbX_3$ perovskite in hexane solution. It can be seen that the absorption spectra of samples with the higher bromine composition stay slightly blue-shifted.

The PL emission spectra of the $CsPbX_3$ perovskite depend on the compositional modulations (different ratio of the PbX_2 salt). Figure 4a shows the optical images of the $CsPbX_3$ samples under the UV light (λ_{ex}=365 nm) while Figure 4b represents the PL emission spectra of the perovskites in hexane solution (λ_{ex}=450 nm). For example, the maximum PL emission peak is 517 nm at an excitation wavelength of 450 nm for the $CsPbBr_3$ perovskite, whereas 700 nm for the $CsPbI_3$

perovskite. The PL emission spectra of other samples with different ratios of Br to I are distributed among 517-700 nm spreading from green light to red light. It confirms that the PL emission wavelength for $CsPbX_3$ perovskites is controlled by composition modulations. On the basis of the reported literatures, [3,10,22] perovskite can be synthesized using the $PbCl_2$ salt to obtain blue PL emission. Thus, the perovskite quantum dots exhibit compositional-tunability through the entire visible spectral region of 410-700 nm. Detailed information of the perovskite samples is provided in Table S2 including the maximum PL emission wavelength, narrow FWHM and QY. The absolute QY of the $CsPbI_3$ reached up to 70% using the integrating sphere method under excitation of 450 nm. For traditional nanoparticles, such as ZnO [25], comprehensive spectral studies are usually considered to be associated with the surface effect. The same is true for the perovskite QDs. According to the literature [24], halogen ions were found to be enriched on surfaces of $CsPbX_3$ QDs, resulting in self-passivation effect on defects, which would greatly reduce non-radiative trappers. It is one of major reasons to achieve the unexpected outstanding luminescence properties of $CsPbX_3$ QDs.

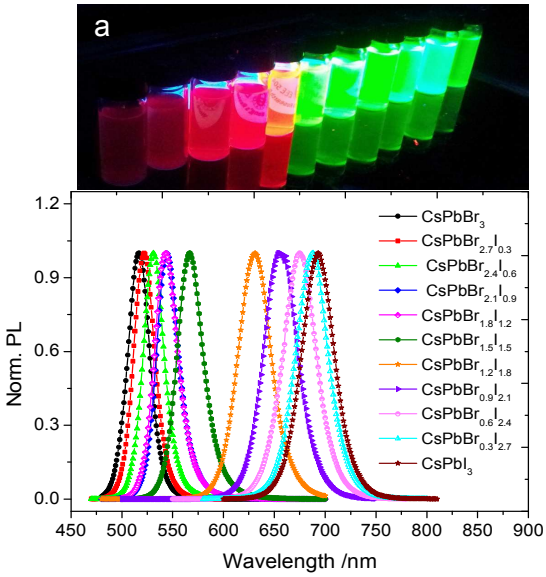

Figure 4: a: The optical images of the perovskites under the UV light (λ_{ex}=365 nm); b: Fluorescence emission spectra of all the $CsPbX_3$ perovskites in hexane solution.

Figure 5: Schematic of the polarization experimental setup. We detected the polarized emission of the perovskite with a collimation light, which has no polarization property.

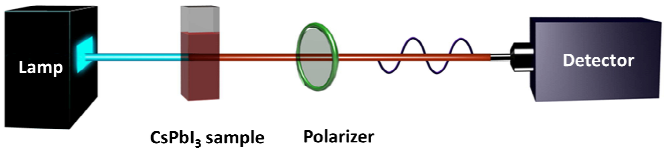

3.3 Polarization Property of the $CsPbX_3$ Perovskite

Surprisingly, the $CsPbX_3$ QDs exhibited polarization property despite in hexane solution or in film form. To our knowledge, the polarization properties have been studied systematically for the first time. The experimental setup is schematically depicted in Figure 5.

$CsPbI_3$ in hexane can be taken as an example to illustrate the polarization property of perovskites. The polarization of a light beam is as follows:

$$P = (I_{max}-I_{min}) / (I_{max}+I_{min}), \quad (1)$$

where I is the intensity of polarized emission after passing through the polarizer. [22] According to Figure 6a, the change of intensity of the polarized emission is almost consistent with the sine function and the polarization is 0.36. Moreover, the polarization of $CsPbI_3$ remained almost unchanged (about 0.34) after 15 days. Figure 6b shows the polarization of all the samples in hexane. We can find that the increasement of iodine amount helps improve the polarization of perovskite. Referring to TEM images and XRD analysis in last section, the $CsPbBr_3$ perovskite belongs to cubic crystal structure while $CsPbI_3$ QDs are distorted from the cubic structure caused by bigger iodine atom. [4,10] The distorted cubic structure breaks the space inversion symmetry and the resulted asymmetrical structure [26] would be responsible for the polarization property of $CsPbX_3$ perovskite. Another possible reason for the polarized emission is that $CsPbX_3$ perovskite is highly ionized, which facilitates self-organization forming ordered packing structure in hexane.

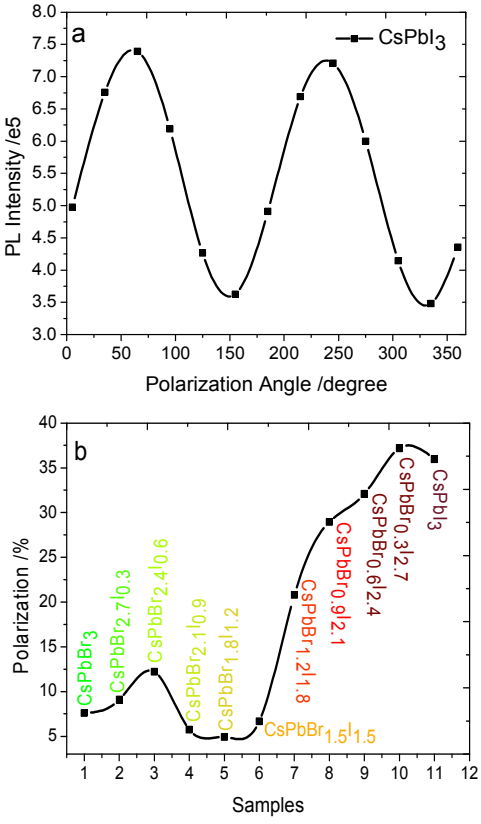

Figure 6: a: Polarization property of the $CsPbI_3$ perovskite in hexane; b: Polarization of all the perovskite samples in hexane.

In an effort to investigate the effect of concentration on

the polarization property, a set of experiment using $CsPbBr_{0.3}I_{2.7}$ QDs at different volume concentration was performed and the results were shown in Figure 7 and Table S4, giving positive results between polarization and concentration. Note the last two samples of $CsPbBr_{0.3}I_{2.7}$ solution were highly diluted, which possibly contributed the drastic reduction of PL intensity especially the 2nd peak of the sine function.

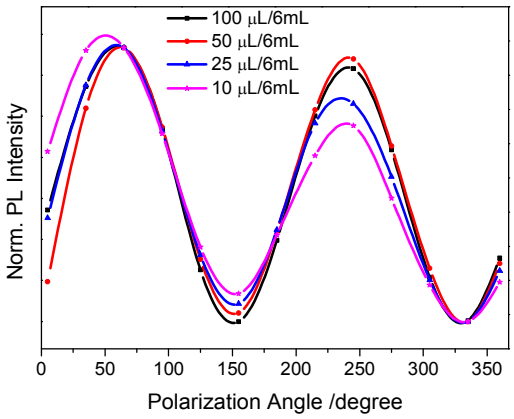

Figure 7: The polarization property of different volume concentration in hexane for the sample of $CsPbBr_{0.3}I_{2.7}$ (VB/V: 100 μL/6 mL; 50 μL/6 mL; 25 μL/6 mL; 10 μL/6 mL).

In addition to the solution, we also have tested the polarization property of perovskite in film form (Figure 8, Figure S4 and Table S5). Figure 8 exhibits the polarization spectra of the $CsPbBr_3$ film and $CsPbI_3$ film. The polarization of $CsPbI_3$ film is as high as 0.40, which is slightly higher than that of $CsPbI_3$ in hexane. The polarization property of perovskite is related to the crystal structure and the degree of order among the perovskite quantum dots. But there is no polarized emission for the $CsPbBr_3$ film at all. From Figure 8, the 2nd peak is significantly lower than the 1st one, indicating a stability issue of $CsPbI_3$ film, which is much lower than the solution form.

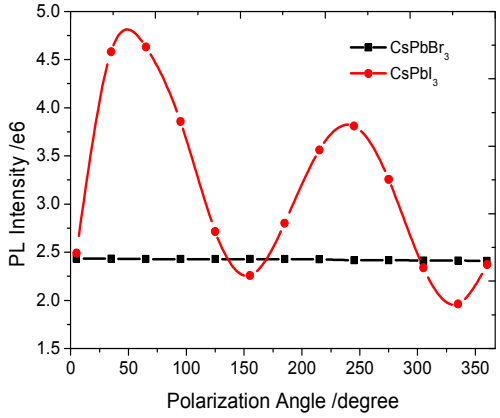

Figure 8: The polarization property of $CsPbX_3$ perovskite in film: Black square dot line: $CsPbBr_3$ film (Left image: Green under the UV light (λ_{ex}=365 nm)); Red circular dot line: $CsPbI_3$ film (Right image: Red under the UV light (λ_{ex}=365 nm)).

There are some other well-known polarized-luminescence materials, such as quantum rods (QRs). Although the polarization of single QR is able to reach as high 0.75 [27], the polarization of QRs solution will dramatically decrease to less than 0.2 due to the random arrangement of quantum rods in solution. To realize polarized emission, QRs need to be aligned by electrospinning, photoinduced alignment, mechanical rubbing, etc. In this study, relative strong polarization of $CsPbX_3$ QDs has been achieved in hexane directly without further alignment processes. There are two major reasons for this phenomenon. Firstly, the polarization is related to the crystal structure of the perovskite. The $CsPbBr_3$ perovskite belongs to cubic crystal structure while $CsPbI_3$ perovskite is distorted from the cubic structure caused by the bigger ionic radius of the iodine atom, which will induce the movement of ionic [4, 10, 28]. Moreover, many previous reports showed that the phenomenon of the movement of ionic species, especially halide ions, does exist in perovskite structure and will induce a reaction towards the change of electronic charge distribution. [28-32] It will break the space inversion symmetry under electric field or the 'built-in' potential of $CsPbX_3$ [33] and produce the dipole moment ($\mu_a=\mu_b\neq\mu_c$) [34] which is responsible for the polarization property of $CsPbX_3$ QDs. Secondly, it may be caused by the spatial arrangement and the degree of order among the individual nanoparticals. [35] As we all know, the distribution of QDs is the random arrangement in solution and the average of polarization will be cancelled out. But for the $CsPbX_3$ QDs, they are attracted to each other and uniformly aligned in a large area named as a cluster and every cluster will result the polarization. The comparison of QDs distribution in TEM is shown in Figure S6. The well-ordered assemblies of perovskite QDs could provide possibilities for the polarization property. [36]

A CIE chromaticity diagram (introduced by the Commission International de L'Eclairage) allows the comparison of the quality of colors by mapping colors visible to the human eye in terms of hue and saturation. Figure 9 shows that the $CsPbX_3$ QDs enjoy a wide color gamut with narrow FWHM, that is, a selected triangle of red, green, and blue emitting $CsPbX_3$ QDs encompasses 103% for the Rec. 2020 standard and 138% for the NTSC standard.

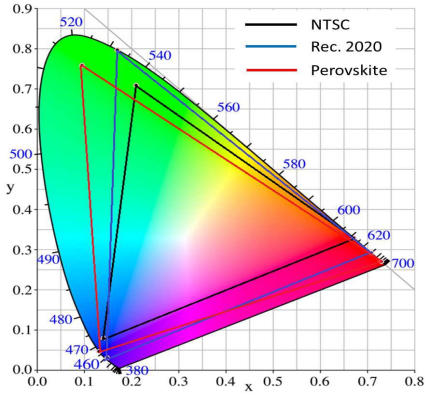

Figure 9: Emission from $CsPbX_3$ QDs (red line) plotted on CIE chromaticity coordinates and compared to most common color standards (NTSC TV and Rec. 2020).

Conclusions

In summary, full inorganic $CsPbX_3$ perovskite QDs have been synthesized using inexpensive precursors. Moreover, the $CsPbX_3$ QDs perform not only excellent photoluminescent but also high polarized emission, which is systematically studied and reported for the first time. The polarization of $CsPbI_3$ reached up to 0.36 in hexane and 0.40 in film. The highly polarized emission from $CsPbX_3$ perovskite promised great potential for low power displays with wide color gamut.

Acknowledgement

This work was supported by National Natural Science Foundation of China (Grant No. 51402148), Guangdong High Tech Project (Grant No. 2014A010105005, No. 2014TQ01C494), Shenzhen Nanshan Innovation Project (Grant No. KC2014JSQN0011A), SUSTC Foundation (Grant No. FRG-SUSTC1501A-48) and Zhonghuan Quantum Co., Ltd.

Notes and references

Department of Electrical & Electronic Engineering, South University of Science and Technology of China, Shenzhen, 518055, P. R. China.
wangk@sustc.edu.cn

1. R. Sheng, X. Wen, S. Huang, X. Hao, S. Chen, Y. Jiang, X. Deng, M. A. Green and A. W. Y. Ho-Bailliea, *Nanoscale,* 2016, **8**, 1926-1931.
2. A. Buin, R. Comin, J.X. Xu, A. H. Ip, and E. H. Sargent, *Chem. Mater.,* 2015, **27**, 4405-4412.
3. L. Dimesso, M. Dimamay, M. Hamburger, W. Jaegermann, *Chem. Mater.,* 2014, **26**, 6762-6770.
4. D. M. Jang, K. Park, D. H. Kim, J. Park, F. Shojaei, H. S. Kang, J. P. Ahn, J. W. Lee, J. K. Song, *Nano Lett.,* 2015, **15**, 5191-5199.
5. O. A. Jaramillo-Quintero, R. S. Sanchez, M. Rincon, I. Mora-Sero, *J. Phys. Chem. Lett.,* 2015, **6**, 1883-1890.
6. H. J. Feng, *J. Power Sources,* 2015, **291**, 58-65.
7. Y. H. Kim, H. Cho, J. H. Heo, T. S. Kim, N. Myoung, C. L. Lee, S. H. Im, T. W. Lee, *Adv. Mater.,* 2015, **27**, 1248-1254.
8. N. K. Kumawat, A. Dey, K. L. Narasimhan, D. Kabra, *ACS Photonics,* 2015, **2**, 349-354.
9. M. Anyi, X. Li, L. F. Liu, Z. L. Ku, T. F. Liu, Y. G. Rong, M. Xu, M. Hu, J. Z. Chen, Y. Yang, H. W. Han, M. Grätzel, *Science,* **345**, 295-297.
10. F. Zhang, H. Zhong, C. Chen, X. G. Wu, X. Hu, H. Huang, J. Han, B. Zou, Y. Dong, *ACS. Nano.,* 2015, **9**, 4533-4542.
11. S. Zhuo, J. Zhang, Y. Shi, Y. Huang, B. Zhang, *Angew Chem. Int. Ed.,* 2015, **54**, 5693-5696.
12. W. Li, J. Li, L. Wang, G. Niu, R. Gao, Y. Qiu, *J. Mater.Chem. A,* 2013, **1**, 11735-11740.
13. C. Law, L. Miseikis, S. Dimitrov, P. Shakya-Tuladhar, X. Li, P. R. Barnes, J. Durrant, B. C. O'Regan, *Adv. Mater.,* 2014, **26**, 6268-6273.
14. I. Chung, B. Lee, J. He, R. P. Chang, M. G. Kanatzidis, *Nature,* 2012, **485**, 486-489.
15. Z. K. Tan, R. S. Moghaddam, M. L. Lai, P. Docampo, R. Higler, F. Deschler, M. Price, A. Sadhanala, L. M. Pazos, D. Credgington, F. Hanusch, T. Bein, H. J. Snaith, R. H. Friend, *Nat Nanotechnol,* 2014, **9**, 687-692.
16. J. Z. Song, J. H. Li, X. M. Li, L. M. Xu, Y. H. Dong, H. B. Zeng, *Adv Mater.,* 2015, **27**, 7162-7167.
17. M. Kulbak, D. Cahen, and G. Hodes, *J. Phys. Chem. Lett.,* 2015, **6**, 2452-2456.
18. H. Zhan, Z. Xu, C. Tian, Y. Wang, M. Chen, W. Kim, Z. Bu, X. Shao, S. Lee, *J. Soc. Inf. Display,* 2014, **22**, 545-551.
19. T. C. Teng and L. W. Tseng, *Opt. Express,* 2014, **22**, 1477-1490.
20. Y. Li, T. X. Wu, and S. T. Wu, J. *Disp. Technol.*, 2009, **5**, 335-340.
21. S. R. Kim, S. W. Lee, *Opt. Eng.,* 2015, **54**, 073111.
22. L. Protesescu, S. Yakunin, M. I. Bodnarchuk, F. Krieg, R. Caputo, C. H. Hendon, R. X. Yang, A. Walsh, M. V. Kovalenko, *Nano Lett.,* 2015, **15**, 3692-3696.
23. B. Philippe, B. W. Park, R. Lindblad, J. Oscarsson, S. Ahmadi, E. M. J. Johansson, H. Rensmo, *Chem. Mater.,* 2015, **27**, 1720-1731.
24. X. M. Li, Y. Wu, S. L. Zhang, B. Cai, Y. Gu, J. Z. Song, and H. B. Zeng, *Adv. Funct. Mater.,* 2016, DOI: 10.1002/adfm.201600109.
25. H. B. Zeng, G. T. Duan, Y. Li, S. K. Yang, X. X. Xu, and W. P. Cai, *Adv. Funct. Mater.,* 2010, 20, 561-572.
26. R. A. M. Hikmet, P. T. K. Chin, D. V. Talapin, H. Weller, *Adv. Mater.,* 2005, **17**, 1436-1439.
27. D. V. Talapin, R. Koeppe, S. Gotzinger, A. Kornowski, J. M. Lupton, A. L. Rogach, O. Benson, J. Feldmann, and H. Weller, *Nano Lett.,* 2003, **3**, 1677-1681.
28. S. Meloni, T. Moehl, W. Tress, M. Franckevicius, M. Saliba, Y. H. Lee, P. Gao, M. K. Nazeeruddin, S. M. Zakeeruddin, U. Rothlisberger, Michael Graetzel, *Nature Communications,* 2015, DOI: 10.1038/ncomms10334.
29. W. Tress, N. Marinova, T. Moehl, S. M. Zakeeruddin, M. K. Nazeeruddin and M. Gratzel, *Energy Environ. Sci.,* 2015, **8**, 995-1004.
30. C. Eames, J. M. Frost, P. R. F. Barnes, B. C. O'Regan, A. Walsh, M. S. Islam, *Nature Communications,* 2015, DOI: 10.1038/ncomms8497.
31. Z. G. Xiao, Y. B. Yuan, Y. C. Shao, Q. Wang, Q. F. Dong, C. Bi, P. Sharma, A. Gruverman and J. S. Huang, *Nature Mater.,* 2015, **14**, 193-198.
32. J. Haruyama, K. Sodeyama, L. Y. Han, and Y. Tateyama, *J. Am. Chem. Soc.*, 2015, **137**, 10048-10051.
33. X. Wang, Y. Chai, L. Zhou, H. Cao, C. D. Cruz, J. Yang, J. Dai, Y. Yin, Z. Yuan, S. Zhang, R. Yu, M. Azuma, Y. Shimakawa, H. Zhang, S. Dong, Y. Sun, C. Jin, Y. Long, *Phys. Rev. Lett.,* 2015, 115-119.
34. Y. Gao, V. D. Ta, X. Zhao, Y. Wang, R. Chen, E. Mutlugun, K. E. Fong, S. T. Tan, C. Dang, X. W. Sun, H. Sun, H. V Demir, *Nanoscale,* 2015, **7**, 6481-6486.
35. B. P. Khanal, E. R. Zubarev, *Angew Chem Int Ed.,* 2007, **46**, 2195-2198.
36. Z. Y. Huo, C. K. Tsung, W. Y. Huang, M. Fardy, R. X. Yan,

X. F. Zhang, Y. D. Li, and P. D. Yang, *Nano Lett.,* 2009, **9**, 1260-1264.